

## SHEAR STABILIZATION OF SOLIDIFICATION FRONTS

S.H. Davis and T.P. Schulze  
Northwestern University  
Department of Engineering Sciences and Applied Mathematics  
Evanston, IL 60208

### ABSTRACT

A linear-stability analysis is performed on the interface formed during the directional solidification of a dilute binary alloy in the presence of a time-periodic flow. In general, the flow is generated by the elliptical motion of the crystal parallel to the interface. The presence of the flow can either stabilize or destabilize the system relative to the case without flow with the result depending on the frequency and amplitude of the oscillations as well as the properties of the material. In particular, we find that the morphological instability present in the absence of flow can be entirely suppressed with respect to disturbances of the same frequency as the oscillation.

### INTRODUCTION

The manufacturing of crystals with uniform material properties is frequently hampered by the presence of morphological instabilities during the solidification of multi-component materials. These nonuniformities result from an interaction between surface morphology and the concentration gradients created by solute rejection. In order to eliminate these nonuniformities, it is necessary to suppress the instability. In the context of directional solidification, this can be done by producing materials with sufficiently low solute concentration, or by controlling the speed of the solidification front<sup>1</sup>.

When it is undesirable to operate within these restricted ranges of parameters, some other method of stabilization is necessary. In the 1960's, Hurle suggested that flow in the melt, either forced or resulting from natural convection, might be used to stabilize the interface. Since then, a number of studies have investigated the effect of various flows on morphological stability.

Delves<sup>2</sup> studied solidification into a Blasius boundary layer, using a parallel-flow approximation. Coriell, McFadden, Boisvert and Sekerka<sup>3</sup> investigated solidification into a plane Couette flow. Forth and Wheeler<sup>4</sup> and Hobbs and Metzener<sup>5</sup> investigated solidification into a parallel flow with the asymptotic suction profile. McFadden, Coriell, and Alexander<sup>6</sup> and Brattkus and Davis<sup>7</sup> looked at solidification into a stagnation point flow. Brattkus and Davis<sup>8</sup> also looked at solidification over a rotating disc. Merchant and Davis<sup>9</sup> studied solidification into a temporally modulated stagnation point flow, and Schulze and Davis<sup>10</sup> considered solidification into a compressed Stokes boundary layer (CSL). For a more extensive review of the role of convection in solidification see Davis<sup>11</sup>.

Here, we follow up on the work studying solidification into a CSL. This flow can be generated by oscillating the crystal parallel to the interface.

### GOVERNING EQUATIONS

We consider the directional solidification of a dilute binary mixture at constant speed  $V$ . We choose a coordinate system with  $x$ -axis located at the mean position of the crystal interface, moving with the front, and a  $z$ -axis that is fixed in the laboratory frame of reference. The equations governing the system in the fluid region are the Navier-Stokes, continuity, and solute diffusion equations:

$$\Omega \mathbf{u}_t + \epsilon \mathbf{u} \cdot \nabla \mathbf{u} - \mathbf{u}_z = -\nabla p + S \nabla^2 \mathbf{u} \quad (2.1)$$

$$\nabla \cdot \mathbf{u} = 0 \quad (2.2)$$

$$\Omega C_t + \epsilon \mathbf{u} \cdot \nabla C - C_z = \nabla^2 C \quad (2.3)$$

$$T = z. \quad (2.4)$$

To simplify the analysis, we neglect latent heat and density changes, and we assume equal densities and thermal properties between the two phases. We also assume that heat diffuses much faster

than solute, and, in this limit, the temperature field is fixed and depends linearly on the vertical coordinate—the frozen temperature approximation<sup>12</sup>. We begin by considering the problem in two dimensions.

We have nondimensionalized the equations by scaling the fluid velocity with the amplitude of the crystal oscillations  $U$ ; the spatial coordinates with the diffusion boundary layer thickness  $D/V$ , where  $D$  is the solute diffusivity; time with the frequency of the crystal oscillations  $\omega$ ; and the temperature and solute concentrations using the product of the diffusion boundary layer thickness and their respective gradients at the interface.

The nondimensional parameters that appear in the equations and boundary conditions are the morphological number  $M$ , the surface energy parameter  $\Gamma$ , the Schmidt number  $S$ , the nondimensional frequency  $\Omega$ , the segregation coefficient  $k$ , and a parameter measuring the amplitude of the lateral oscillations  $\epsilon$ .

$$M = \frac{mVC_{\infty}(1-1/k)}{GD} \quad (2.5)$$

$$\Gamma = \frac{T_m \gamma V}{DL_V m C_{\infty} (1-1/k)} \quad (2.6)$$

$$S = \frac{\nu}{D} \quad (2.7)$$

$$\Omega = \frac{\omega D}{V^2} \quad (2.8)$$

$$\epsilon = \frac{U}{V} \quad (2.9)$$

Here  $m$  is the liquidus slope in the phase diagram of the binary mixture,  $C_{\infty}$  is the far-field solute concentration,  $G$  is the thermal gradient,  $T_m$  is the melting temperature of the solvent,  $\gamma$  is the surface free energy,  $L_V$  is the latent heat per unit volume, and  $\nu$  is the kinematic viscosity.

The interfacial conditions, evaluated at  $z = h(x, y, t)$  are as follows:

$$u = \cos t \quad (2.10)$$

$$w = 0 \quad (2.11)$$

$$C = M^{-1}h - 2\Gamma H \quad (2.12)$$

$$[1 + \Omega h_t + \epsilon \cos t h_x][1 + (k-1)C] = C_z - C_x h_x, \quad (2.13)$$

where  $H$  is the mean curvature of the interface.

The basic state for this system takes the form

$$\bar{u} = e^{-Bz} \cos(t - Az) \quad (2.14)$$

$$\bar{w} = 0 \quad (2.15)$$

$$\bar{C} = 1 - e^{-z} \quad (2.16)$$

$$\bar{h} = 0, \quad (2.17)$$

where  $A$  and  $B$  are known real constants that depend on the Schmidt number and forcing frequency.

To analyse the response of this state to infinitesimal perturbations, we disturb each of these quantities, and separate the disturbances into normal modes of the form

$$\phi = \bar{\phi} + \hat{\phi}(z, t) e^{i\alpha x} e^{\sigma t} + c.c. \quad (2.18)$$

Here we are seeking time-periodic eigenfunctions with the same period as the basic state, and  $\sigma$  is the Floquet exponent. If the real part of  $\sigma$  is not zero, then the disturbances will experience a net growth or decay over one period.

Routine algebraic manipulations result in two linearized disturbance equations for the solute concentration and vertical component of the velocity.

## SMALL AMPLITUDE OSCILLATIONS

In this section we find conditions on the morphological number  $M$  such that the system is neutrally stable in the limit of small forcing,  $\epsilon \rightarrow 0$ . In this limit, we find that  $\sigma = 0$  on the neutral curve, and we expand the inverse morphological number as

$$M^{-1} = M_0 + \epsilon^2 M_2 + \dots, \quad (3.19)$$

where  $M_0$  corresponds to the no-flow, or Mullins and Sekerka, result.

In Figure 1 we plot the correction to the no-flow result for the CSL as a function of the disturbance wavenumber for various forcing frequencies. If  $M_2 < 0$  for a given wavenumber, a disturbance with that wavenumber will be stabilized relative to the case with no flow. Notice that for  $\Omega = 1$  all finite wavelengths are stabilized. The Schmidt number and segregation coefficient have been chosen to represent a lead-tin alloy for all of the figures in this paper.

In Figure 2 we map out the regions of the  $\alpha$ - $\Omega$  plane where the flow has a stabilizing influence on the interface ( $M_2 < 0$ ). Notice that there is a range of frequencies for which all finite wavenumbers are stabilized. We refer to this as a *window of stabilization*.

It turns out that the CSL is only able to stabilize in two dimensions. In three dimensions, only disturbances with wavevectors aligned with the parallel flow will be stabilized while those with wavevectors perpendicular to the flow are unaffected—thus the flow acts as a pattern selection mechanism only.

## SMALL AMPLITUDE NONPLANAR OSCILLATIONS

Motivated by the work of Kelly and Hu<sup>13</sup> on Benard convection, we attempt to extend the stabilizing influence of the CSL to three dimensions by considering the influence of nonplanar oscillations. Specifically, we consider the effect of adding a second oscillation perpendicular to the first which has the same frequency, but may differ in amplitude and phase. This corresponds to translating the crystal in elliptical orbits parallel to the interface.

For the correction due to a weak flow, we get

$$M_2 = [(\cos \theta + \lambda \cos \gamma \sin \theta)^2 + \lambda^2 \sin^2 \theta \sin^2 \gamma] M_2^{(2D)}, \quad (4.20)$$

where  $M_2^{(2D)}$  is the result for oscillations in one direction only (CSL),  $\theta$  is the angle that the disturbance wave vector makes with the x-axis,  $\lambda$  is the amplitude ratio of the oscillations, and  $\gamma$  is the phase difference between the oscillations.

If the two oscillations are either perfectly in or out of phase (corresponding to a phase angle that is an integral multiple of  $\pi$ ), there will be some  $\theta_c$  for which the correction to the no-flow result,  $M_2$ , is zero. This means that the flow will be able to destabilize the interface if  $M_2^{(2D)} > 0$ , but acts only as a pattern selection mechanism if  $M_2^{(2D)} < 0$ , with disturbances oriented at the angle  $\theta_c$  being the least stable. This is a degenerate case corresponding to a single oscillation along an axis lying in the x-y plane. The result is therefore equivalent to that for the CSL.

When the phase between the oscillations,  $\gamma$ , is not a multiple of  $\pi$ , the factor appearing in front of  $M_2^{(2D)}$  is positive, and it is possible to stabilize an arbitrary three-dimensional disturbance provided  $M_2^{(2D)} < 0$ . Thus the ability of the nonplanar oscillations to stabilize the interface is predicted by the results for the CSL, and the window of stabilization is the same for both cases.

The maximum stabilization occurs when the phase angle is  $\pi/2$ , with the stabilization being greater along whichever axis has the largest amplitude oscillations. If the amplitude ratio,  $\lambda$ , is one, there will be no preferred direction for cell orientation.

## FINITE AMPLITUDE OSCILLATIONS

In the previous section we showed that some degree of stabilization can be achieved by using small-amplitude nonplanar oscillations with a frequency lying within a given range. In this section we show that the Mullins and Sekerka interfacial mode can be entirely suppressed if these oscillations have sufficiently large amplitude.

Following the method used by Hall<sup>14</sup> for the Stokes layer, we find an exact solution for our system in the form of a Fourier series in time. We then truncate this series to produce numerical results.

In Figure 3 we plot  $M^{-1}$  versus  $\alpha$  for a forcing frequency  $\Omega = 10$ , which lies within the window of stabilization, and we see that by taking epsilon sufficiently large we can force the neutral curve below the x-axis. In Figure 4 we plot  $M^{-1}$  versus  $\epsilon$  for the same frequency and with the wavenumber fixed at the critical value for the instability in the absence of flow. Notice that when  $\epsilon$  exceeds about 60, the instability is completely suppressed.

## CONCLUSION

We have found that nonplanar oscillations of the crystal during directional solidification can be used to entirely suppress the Mullins and Sekerka instability provided the frequency of these oscillations is within a given range and that their amplitude is sufficiently large. We have found that this window of stabilization persists for a wide range of material parameters and operating conditions.

We have searched for other modes of instability, especially subharmonics, but have not located any. If there are no other modes of instability, the modulation proposed here may provide a practical means for stabilizing the interface during directional solidification.

## References

- <sup>1</sup> Mullins, W.W. and Sekerka, R.F., *J. Appl. Phys.* **35** (1964) 444.
- <sup>2</sup> Delves, R.T., *J. Cryst. Growth* **8** (1971) 3.
- <sup>3</sup> Coriell, S.F., McFadden, G.B., Boisvert, R.F. and Sekerka, R.F., *J. Cryst. Growth* **69** (1984) 15.
- <sup>4</sup> Forth, S.A. and Wheeler, A.A., *J. Fluid Mech.* **202** (1989) 339.
- <sup>5</sup> Hobbs, A.K. and Metzener, P., *J. Cryst. Growth* **112** (1991) 539.
- <sup>6</sup> McFadden, G.B., Coriell, S.R. and Alexander, J.I.D., *Commun. Pure Appl. Math.* **41** (1988) 683.
- <sup>7</sup> Brattkus, K. and Davis, S.H., *J. Cryst. Growth* **87** (1988) 385.
- <sup>8</sup> Brattkus, K. and Davis, S.H., *J. Cryst. Growth* **89** (1988) 423.
- <sup>9</sup> Merchant, G.J. and Davis, S.H., *J. Cryst. Growth* **96** (1989) 737.
- <sup>10</sup> Schulze, T.P. and Davis, S.H., *J. Cryst. Growth* (in press).
- <sup>11</sup> Davis, S.H., in *Handbook of Crystal Growth*, edited by D.T.J. Hurle, North-Holland (1993).
- <sup>12</sup> Langer, J.S. *Rev. Mod. Phys.* **52** (1980) 1.
- <sup>13</sup> Kelly, R.E. and Hu, H.-C., *J. Fluid Mech.* **249** (1993) 373.
- <sup>14</sup> Hall, P., *Proc. Roy. Soc. Lond. A.* **359** (1978) 151.

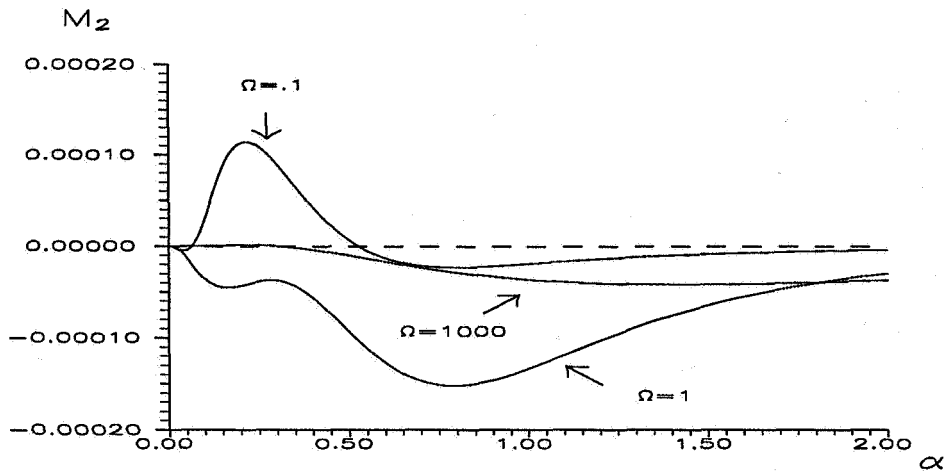


Figure 1:  $M_2$  vs.  $\alpha$  for  $S = 81.0$ ,  $k = 0.3$  and various  $\Omega$ .  $M_2$  is independent of  $\Gamma$ . When  $M_2$  is above the x-axis, the influence of the flow is destabilizing, and when  $M_2$  is below the x-axis, the influence of the flow is stabilizing. As  $\Omega \rightarrow \infty$ ,  $M_2 \rightarrow 0$ , and as  $\Omega \rightarrow 0$ ,  $M_2$  approaches a steady state. Note that for  $\Omega = 1$  the flow is stabilizing for all wavenumbers.

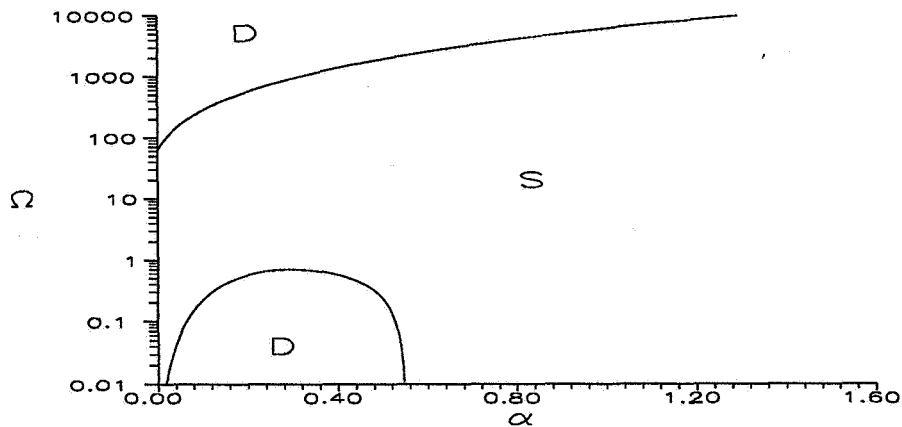


Figure 2: **Directional solidification into Stokes layer:** Regions of the  $\alpha$ - $\Omega$  plane where the flow stabilizes (S) or destabilizes (D) the interface relative to the case without flow.  $S = 81.0$  and  $k = 0.3$ ; result is independent of  $\Gamma$ .

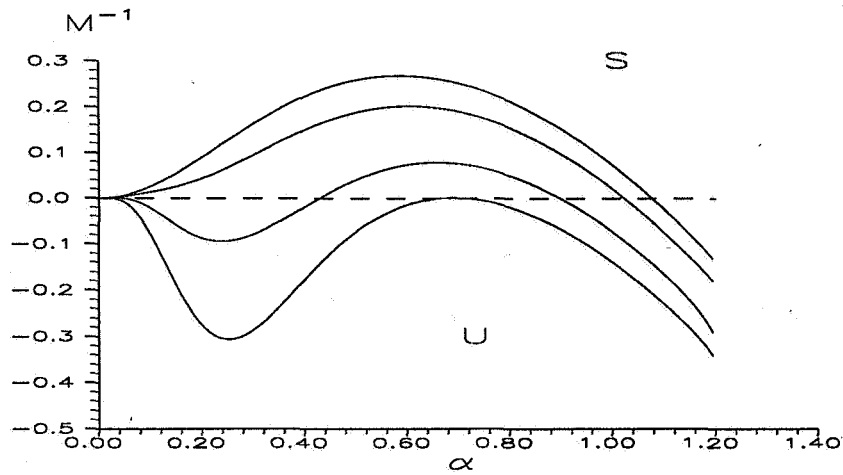


Figure 3:  $M^{-1}$  vs.  $\alpha$  for  $k = 0.3$ ,  $S = 81.0$ ,  $\Omega = 10.0$ , and  $\epsilon = \{0, 20, 40, 60\}$ . As  $\epsilon$  is increased the flow stabilizes the interface, and for  $\epsilon \approx 60$  the Mullins and Sekerka interfacial instability is entirely suppressed.

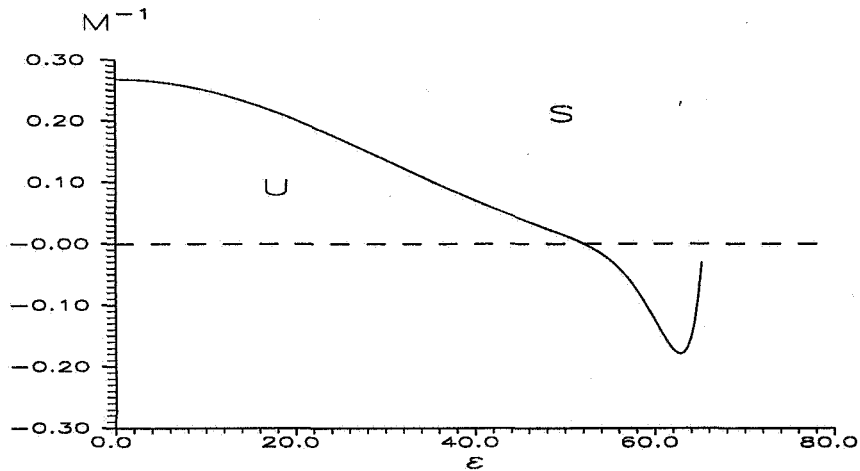


Figure 4:  $M^{-1}$  vs.  $\epsilon$  for  $k = 0.3$ ,  $S = 81.0$ ,  $\Omega = 10.0$ , and  $\alpha$  fixed at the critical value for the no-flow system. Notice that the stabilizing trend begins to reverse if the amplitude of the flow oscillations is too great.